RESULTS OF LABORATORY EVALUATION OF STARING ARRAYS

APRIL 18, 1990

CURTIS M. WEBB

CENTER FOR NIGHT VISION AND ELECTRO-OPTICS
FORT BELVOIR, VA 22060

ABSTRACT

This paper will present the results obtained at the Center For Night Vision and Electro-Optics of laboratory measurements of staring array thermal imaging systems. The results that will be reported are a compilation of a number of different systems tested. This data will be utilized not so much as a presentation of system performance but to show the relevance and validity of the tests. It is hoped that through the presentation of this data the thermal imaging community will get a better understanding of both laboratory and field performance of staring array thermal imaging systems.

2. INTRODUCTION

Present FLIR technology is rapidly heading towards systems that use discretely sampled staring arrays to take advantage of their durability and relative low cost. With these changes arise some very interesting problems in the laboratory evaluation of these systems. Laboratory evaluations including Minimum Resolvable Temperature Difference (MRTD) and Modulation Transfer Function (MTF) and Noise Equivalent Temperature Difference (NETD) have long been performed using methods derived and accepted for scanning thermal imagers. The results that have been obtained from these laboratory measurements have been different than what has been obtained for scanning systems. This paper will present some of the results of the measurements that have been performed at the Center For Night Vision and Electro-Optics.

2. MINIMUM RESOLVABLE TEMPERATURE DIFFERENCE (MRTD)

It is widely known and documented that systems discretely sampled in both the vertical and horizontal direction have limits of resolution dictated by 1/2 the sampling frequency (Nyquist).[1] This happens because at frequencies significantly higher than 1/2 the sampling rate there are not enough samples across the pattern to reproduce that pattern. Because of the phase effects, the MRTD is a function of the relationship between the bars and the detectors. Complete representation of the MRTD is not just one curve but a family of curves for differing phase relationship of the target and detectors.

2.1 Test setup and procedures

The FLIRs used for the following analysis were two separate Mitsubishi Thermal Imaging Cameras model IR-5120A with 512x512 element PtSi Schottky-barrier Focal Plane Arrays (FPA). The detector element size was 26um(H)x20um(V) with a detector area of 203um. Both systems were equipped with an f/1.2 50mm lens which resulted in an Instantaneous Field of View (IFOV) of about 0.50 milliradians.

A first series of MRTD tests were done on one Mitsubishi model IR-5120A to determine the effects of sampling on the MRTD curve. This test consisted of presenting 7:1 aspect ratio MRTD targets to the imager at increasingly higher spatial frequencies. Phase relationship of the bars and detectors were varied for each spatial frequency. An MRTD value was obtained for each target at several different phases. For this discussion phase is referenced to the detector, hence a shift in phase of 180 degrees would result from a displacement of a target 1/2 the distance of the detector IFOV. The setup consisted of a target wheel with several MRTD targets mounted on a translation stage. The target wheel was positioned at the object plane of a 120 inch focal length collimator. The translation stage had a minimum step size of 0.0001 inches which equates to 0.00083 milliradians. This allowed for very accurate positioning of the targets across the full range of phase. Optimum phase position was determined before the MRTD was obtained for each target. This was done by moving the target across the field of view and determining subjectively the position that provided the best representation of the four bars. MRTD values were then obtained at this position and subsequent increments of 90 degrees phase. The MRTD value was then obtained for this point by slowly decreasing the temperature until the point at which the bars first appear as black bars while operating the FLIR in the white hot mode. Then the temperature was slowly incremented until the point at which all four bars were resolvable as white bars. The target was only considered resolvable when all four bars were resolvable. The MRTD value was then recorded as the 1/2 the difference between these two values. This was then repeated for each increment of

phase and for all targets up to the Nyquist point.

Figure 1 shows the results of the MRTD tests that were performed. The primary objective was to show the effects of phase and sampling on the MRTD curve. As expected, the MRTD curve is higher at phase values other then the best phase. The interesting portion of this curve are those MRTD values obtained above 0.7 of Nyquist. Up to about 0.7 cy/mrad or 0.7 of Nyquist the curve behaves expectedly, increasing asymptotically. At frequencies above 0.8 of Nyquist the curve drops and reaches a minimum at Nyquist then asymptotes just above the Nyquist value. The shape of this MRTD curve is very characteristic of those seen for most other staring array FLIRs.

The rationale for the decrease in the MRTD values above 0.85 of Nyquist can be explained by referring to figures 2 through 4. Figure 2a illustrates a single row of detectors and a four bar pattern of frequency 1/4 the sampling frequency or 1/2 the Nyquist rate. Figure 2b represents the resultant of the convolution process between the detector and the periodic bar pattern multiplied by the number of detectors in the array row. By then convolving Figure 2b with a Gaussian spread function and allowing for a shift in level above background would result in an output signal in volts seen in figure 2d. Mathematically, this is represented as[2];

$$Q(X) = [[R(X) * H(X)]S(X)] * G(x) \qquad \text{eq. 1}$$

where R(X) denotes the response as a function of X across a detector, H(X) represents the input bar pattern, S(X) represents the sampling frequency and G(X) is a Gaussian spread function whose half width is equal to d, the system Instantaneous Field of View (IFOV). This same convolution process has been done in figure 3 for a target of frequency 0.87 of Nyquist. Figures 3d and 3h represent the output seen by an observer for two different phase orientations.

MRTD has be defined as the lowest temperature which allows for resolution of all four bars. From figure 3 it is shown that the bar/space pair that limits resolution of the four bar pattern is that pair which we have defined as the Critical Bar Signal[3]. The Critical Bar Signal is the bar/space pair which provides the lowest peak-to-valley signal in volts. It follows that the contrast difference of the Critical Bar Signal must be greater then the contrast threshold of the human observer to provide for resolution of the entire bar pattern.

Figure 4 shows this same convolution process for the bar pattern equal to the Nyquist frequency. Figure 4a shows the bar pattern in perfect phase with the detector array. Thus, convolution with the Gaussian spread function results in an output

signal seen in figure 4d. This figure shows no difference in signal between all the bar/space pairs. The signal is thus limited only by the convolution with the Gaussian spread function and not by the convolution of the signal with the sampled detector array. This is also the case for targets below 0.7 of Nyquist where the Critical Bar Signal for all bar/space pairs of a target are the equal.

Comparison of the figures 3 and 4 show the Critical Bar Signal of the bar pattern at the Nyquist rate (figure 4) to be greater than that of the lower spatial frequency pattern in figure 3. It follows that the optimum phase MRTD of the higher spatial frequency target will have a lower MRTD when compared to some targets at lower spatial frequency.

For frequency of bars equal to the Nyquist frequency, great care must be taken to assure that the bars are in perfect phase with the detectors. Unlike the lower frequency targets which provide representation of the four bars at phases other then zero, the reproduction of the bars at the Nyquist frequency only occurs when the bars are in perfect phase. This results in the inability to resolve the pattern at Nyquist frequency for phases other than the optimum phase. This explains the cutoff of the 180 degree phase MRTD curve shown in figure 1.

3. CONTRAST TRANSFER FUNCTION

To better understand the effects of the sampling a Contrast Transfer Function (CTF) test was performed on the system. This helped to explain the uncharacteristic shape of the MRTD curve. The CTF measurement consists of recording the modulation contrast of the output of a system as a function of spatial frequency. The Modulation Transfer Function (MTF) assumes the system output to be linear and isoplanatic. The CTF considers the shift variance of the image that is characteristic of a sampled signal. Bradley and Dennis[4] have described a method of obtaining the CTF or image contrast of a staring array as:

$$\text{image contrast} = \frac{S1 - S2}{S1 + S2} \qquad \text{eq. 2}$$

where S1 and S2 are the maximum and minimum values of what we have defined as the Critical Bar Signal. Figure 5 shows the results of the CTF test. Clearly from this figure there is a definite dip in the CTF at frequencies between 0.65 and 0.95 of Nyquist. This correlates to the increase in MRT for these frequencies as seen in figure 1. It was noted that the amount of dip in the CTF curve was dependent on the temperature difference of the bars and background. The greater the temperature differ-

ence resulted in a less pronounced dip in the CTF. The curve shown in figure 5 was obtained with a temperature just slightly higher then the highest temperature needed to resolve any of the MRTD targets. This resulted in a substantial dip in the CTF curve. The CTF curve ends at the Nyquist value because we have limited the CTF to the modulation contrast that provides complete four bar reproduction. At frequencies higher then Nyquist the frequencies aliased and thus did not provide a true representation of the original frequency. The aliasing will result in the four bars being reproduced as anything from three bars to no bars.

The dip in the CTF curve results from the system being contrast limited at these frequencies due to nonisoplanatic effects of the sampling. The regions not effected by the contrast limits exhibit the shape of the MTF of the optics, electronics and detectors. Hence, it can be said that all spatial frequencies that provide varying bar/space signals for a given target will result in the MRT being affected not only by the MTF of the system but also the CTF of the system.

4. NOISE ANALYSIS

The final tests to be discussed is a full characterization of noise for a staring array. Conventional methodology for the analysis of Noise Equivalent Temperature Difference (NETD) has strictly dealt with the temporal noise in the horizontal direction. It was assumed that the temporal noise in the vertical direction was the same. In addition, spatial noise in both the horizontal and vertical direction were ignored. We will now discuss a method of acquiring and analyzing both the temporal and spatial noise for the vertical and horizontal direction for a staring array.[5] This methodology was first developed for improved treatment of scanning systems.

The analysis of vertical and horizontal noise for a staring array will be broken into seven components for each orientation. A convenient notation has been adopted which can be used to identify specific noise components. Subscripts are used to show the spatial and temporal regimes over which a specific noise component exists. For example N_{TVH} indicates a noise component which exists over time and in both vertical and horizontal directions (temporal bidirectional). N_{TV} indicates noise which exists over time and in the vertical direction only (temporal vertical). By definition N_{TV} is totally correlated in the horizontal direction (no noise variation in that direction). Summary quantities consisting of more than one type of component are designated using multiple subscripts. For example $N_{TVH,TV}$ indicates a noise quantity consisting of the two noise types discussed above (total temporal vertical).

The components for the vertical noise analysis are listed below:

- Total Spatial Vertical ($N_{VH,V}$)
- Total Temporal Vertical ($N_{TVH,TV}$)
- Total Vertical Noise ($N_{TVH,TV,VH,V}$)
- Spatial Vertical (N_V)
- Temporal Vertical (N_{TV})
- Temporal Bidirectional (N_{TVH})
- Spatial Bidirectional (N_{VH})

This discussion will be limited to the analysis of the vertical noise to include the two bidirectional components N_{TVH} and N_{VH}. Horizontal noise can be analyzed in a similar manner.

Figure 6 illustrates the process used to obtain these noise components for the vertical orientation. Two sets of data for a given set of video lines are obtained. The first set, defined as the noise set, consist of a single line of a field acquired from a digitizer. This is the signal which contains all components of the noise including the temporal and the spatial for a video line. The second set, defined as the background set, consists of the same video line averaged over approximately 256 consecutive frames. This is done to average out the temporal noise from the video line and leave the spatial noise. Both sets of data are acquired for multiple lines of the field of view. The data is then arranged into column form by isolating the corresponding data points from each video line set acquired above.

At this point the Total Temporal Vertical Noise ($N_{TVH,TV}$) can be obtained by subtracting a desired column in the background array set from the corresponding column in the noise set. This is done to subtract out the spatial noise caused by the line-to-line nonuniformity of the image. What remains after this subtraction is the total temporal noise from line to line for a given column. The Root Mean Square (RMS) is then calculated on the resulting column and NETD for that noise component is derived.

The Total Spatial Noise ($N_{VH,V}$) is obtained by first applying a curve fit to a desired column of the background array set thus effectively integrating out local spatial noise. This curve fit data is then subtracted from the corresponding column of the background array set. This is done to subtract out the large area nonuniformity. What remains is the pure spatial noise caused by the line-to-line nonuniformity.

The Total Vertical Noise ($N_{TVH,TV,VH,V}$) is the total of the spatial and temporal noise of the system which exists in the vertical direction. This is obtained by curve fitting a column

from the background set and subtracting that from the corresponding column in the noise set. What will remain after this subtraction is all the noise including the total spatial and temporal noise. RMS is calculated on the result of the subtraction and NETD is obtained for Total Vertical Noise.

The Spatial Vertical Noise (N_V) is the fixed line-to-line non-uniformity in the system that arises because of gain and offset non-uniformity in the focal plane and processing electronics. For a staring array the primary contributor to this noise is the noise from the electronics and not the focal plane. This is obtained by averaging the data points of each horizontal row of the background and noise set to obtain a one dimensional array which contains the average of each horizontal row with N_{TVH} and N_{VH} removed by the horizontal averaging. The one dimensional array which is derived from this is a vertical column of all the averages of the horizontal rows. Figure 7 illustrates this concept. A curve fit of the background, row averaged, single column is again performed. The curve fit column is then subtracted from the background, row averaged, single column and the RMS is obtained. NETD is the calculated.

The Temporal Noise (N_{TV}) is the temporally changing line-to-line variations in the vertical direction. This noise arises primarily because of low frequency (1/f) detector and electronic noise. This is measured by using the same data obtained in the Spatial Noise discussion above. The one dimensional array containing the background row averaged column is subtracted from the noise, row averaged column and RMS and NETD are derived.

The Bidirectional Temporal Noise (N_{TVH}) is the subtraction of the Temporal Vertical Noise (N_{TV}) from the Total Temporal Vertical Noise($N_{TVH,TV}$). This is obtained from the following equation:

$$N_{TVH} = \sqrt{(N_{TVH,TV})^2 - (N_{TV})^2} \qquad \text{eq. 3}$$

The Bidirectional Spatial Noise (N_{VH}) is the subtraction of the Spatial Vertical Noise (N_{VH}) from the Total Spatial Vertical Noise ($N_{VH,V}$). This is obtained from equation 4.

$$\therefore \quad N_{VH} = \sqrt{(N_{VH,V})^2 - (N_V)^2} \qquad \text{eq. 4}$$

The Bidirectional terms N_{TVH} and N_{VH} should be the primary limiting noise components for the staring array. These terms are presently being implemented into the MRTD module of the C2NVEO Advanced FLIR Systems Performance Model and will be used to better predict the field performance of staring arrays.

5. CONCLUSION

The effects of sampling not only affect the resolution of discretely sampled staring arrays but in addition it has been shown that sampling also affects the sensitivity of the system and thus the shape of the MRT curve. It has been shown that the Minimum Resolvable Temperature Difference of staring arrays are not just limited by Nyquist or the MTF of the system but also what we have defined as the Critical Bar Signal. A new concept in the evaluation of noise for a scanning and staring arrays has been introduced. This process will include the evaluation of temporal and spatial noise for both horizontal and vertical directions.

6. ACKNOWLEDGMENTS

The author would like to take this opportunity to acknowledge and thank John D'Agostino for his contribution and help on the concept and design of the noise analysis.

7. REFERENCES

(1)D.F. Barbe,S.B. Campana;"Imaging Arrays Using The Charge-coupled Concept", in Advances in Image Pickup and Display, Vol.3 1977

(2)D.F. Barbe, S.B. Campana; "Imaging Arrays Using The Charge-Coupled Concept", in Advances In Image Pickup and Display, Vol.3 1977, pp. 241

(3)Private conversation with Mel Friedman, 2/14/90

(4)D.J. Bradley and P.N.J. Dennis, "Sampling Effects In CdHgTe Focal Plane Arrays",SPIE Vol. 590, 1985, pp 53-60

(5) L. Scott, L. Condiff, C2NVEO Advanced FLIR Systems Performance Model, SPIE Technical Symposium, 1990

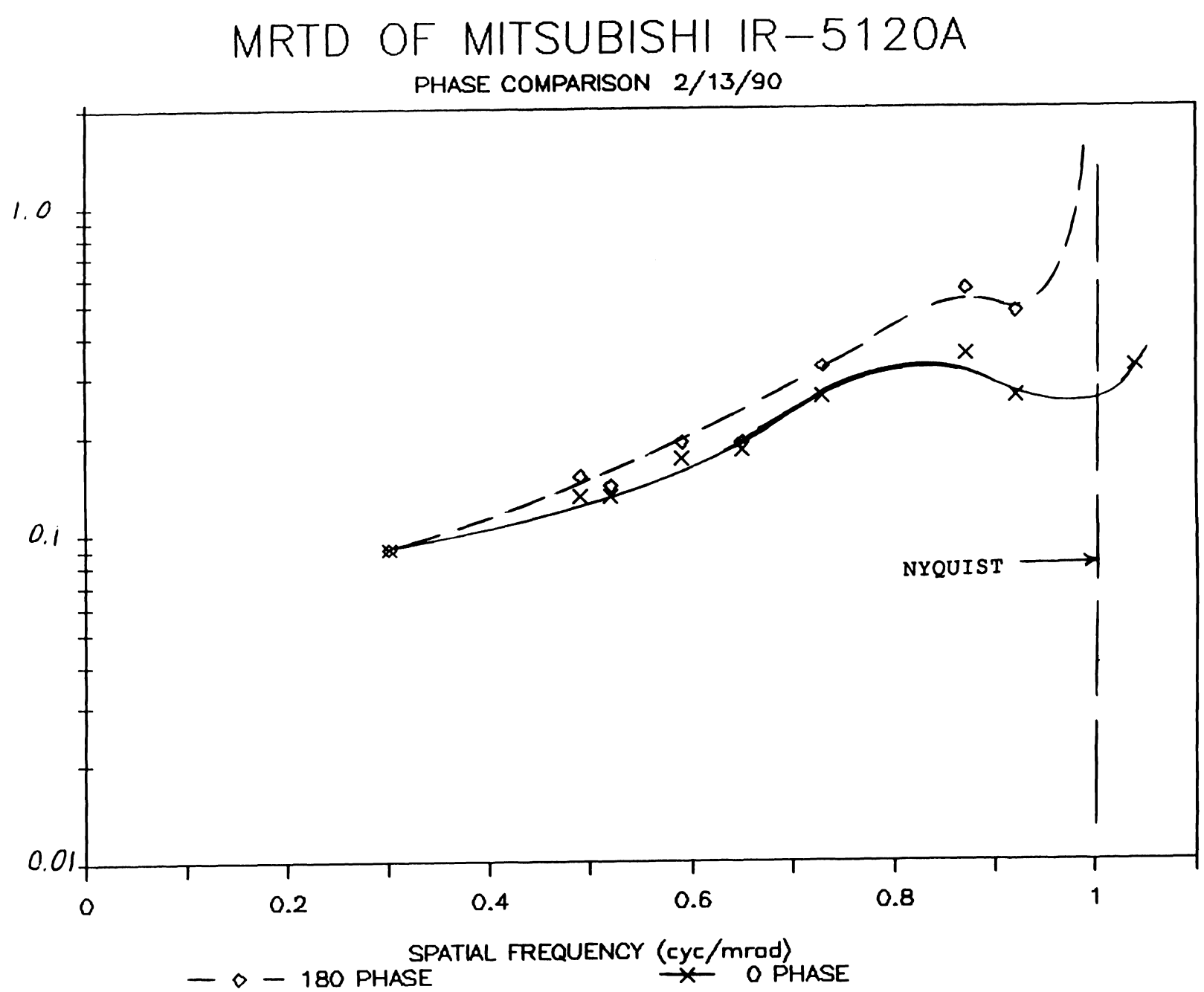
MRTD OF MITSUBISHI IR-5120A
PHASE COMPARISON 2/13/90
1.0
0.1
0.01
0
0.2
0.4
0.6
0.8
1
NYQUIST
SPATIAL FREQUENCY (cyc/mrad)
180 PHASE
0 PHASE

$f = \frac{1}{2} f_N$

Figures 2A-D

$f = \frac{1}{4} f_s$

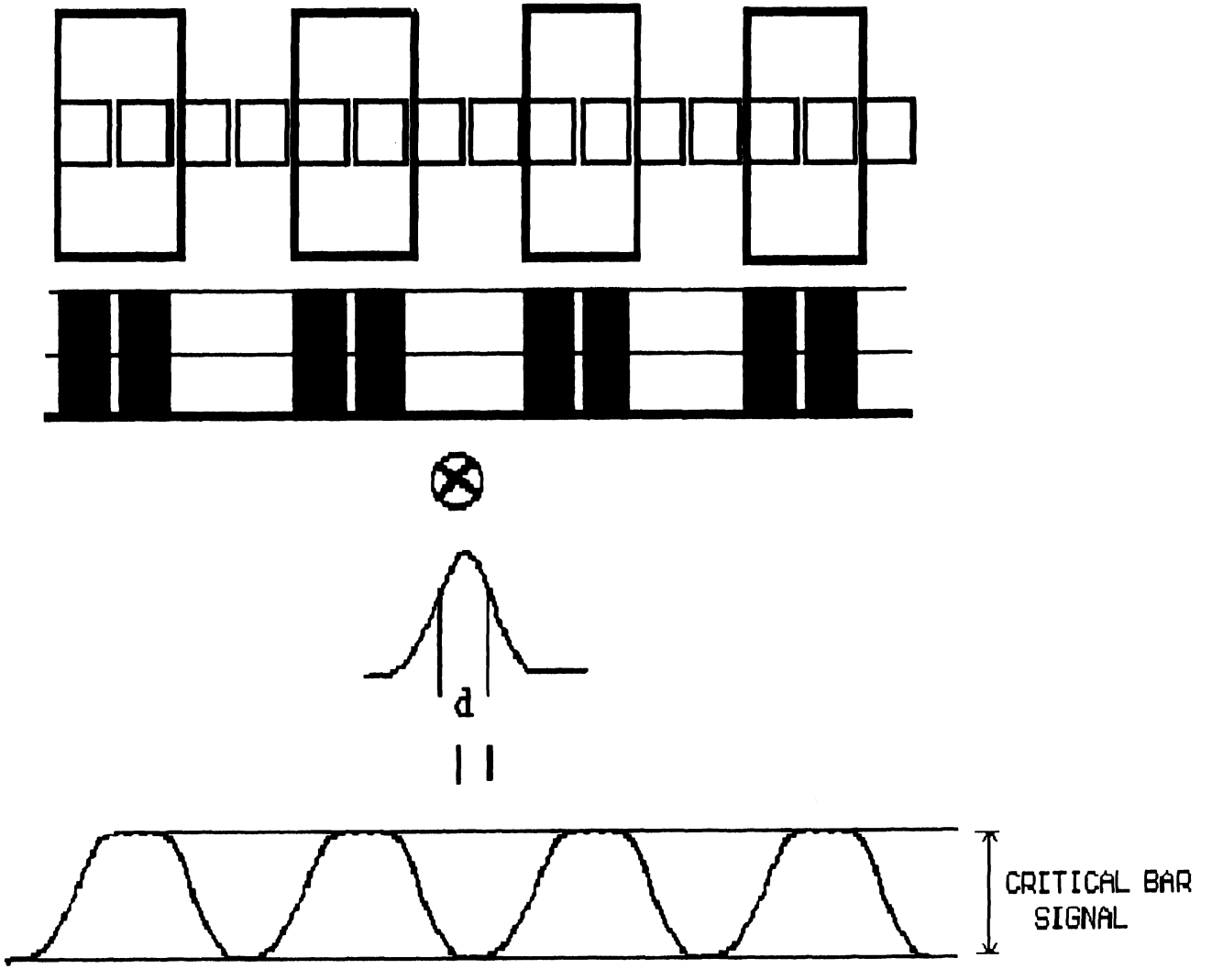

$f = .87\, f_N$

Figures 3A-H

$f = \frac{1}{2.3} f_s$

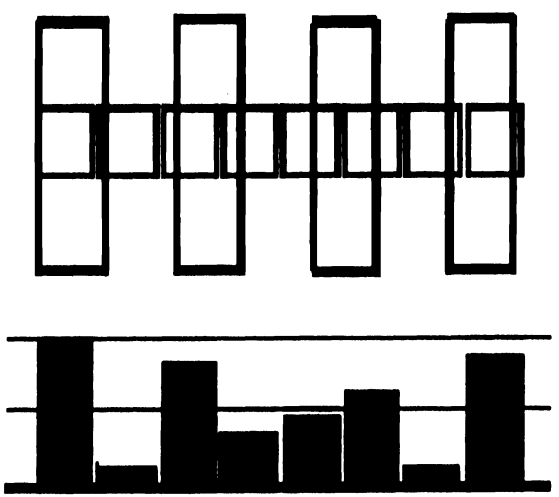

Figure 3A-B

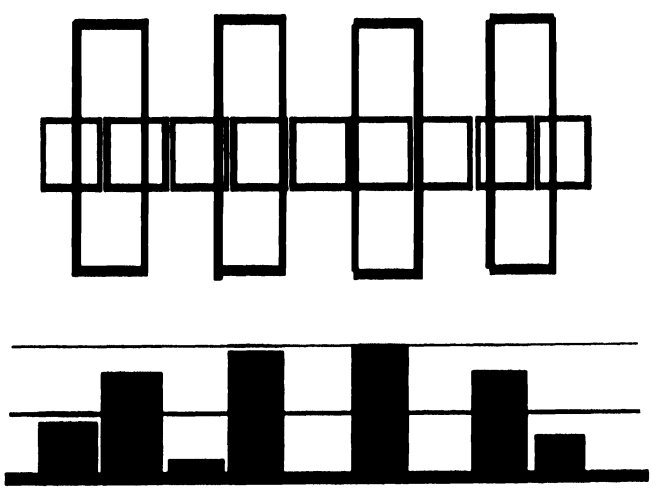

Figure 3E-F

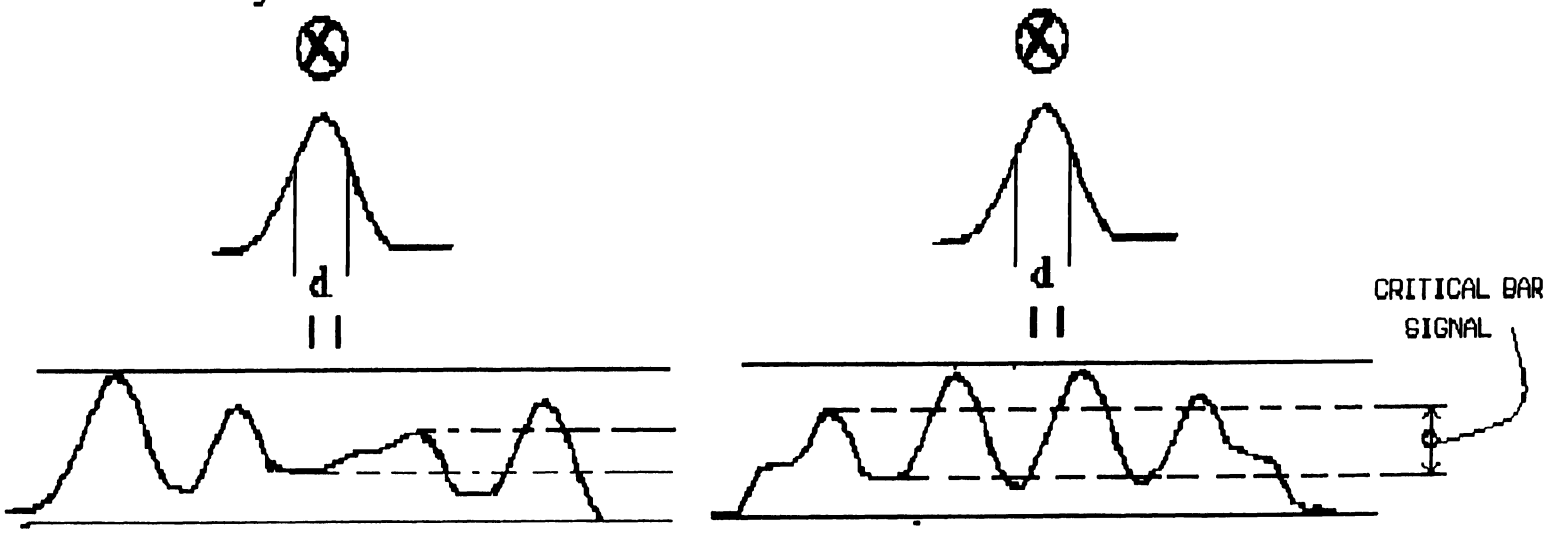

Figures 4A-D

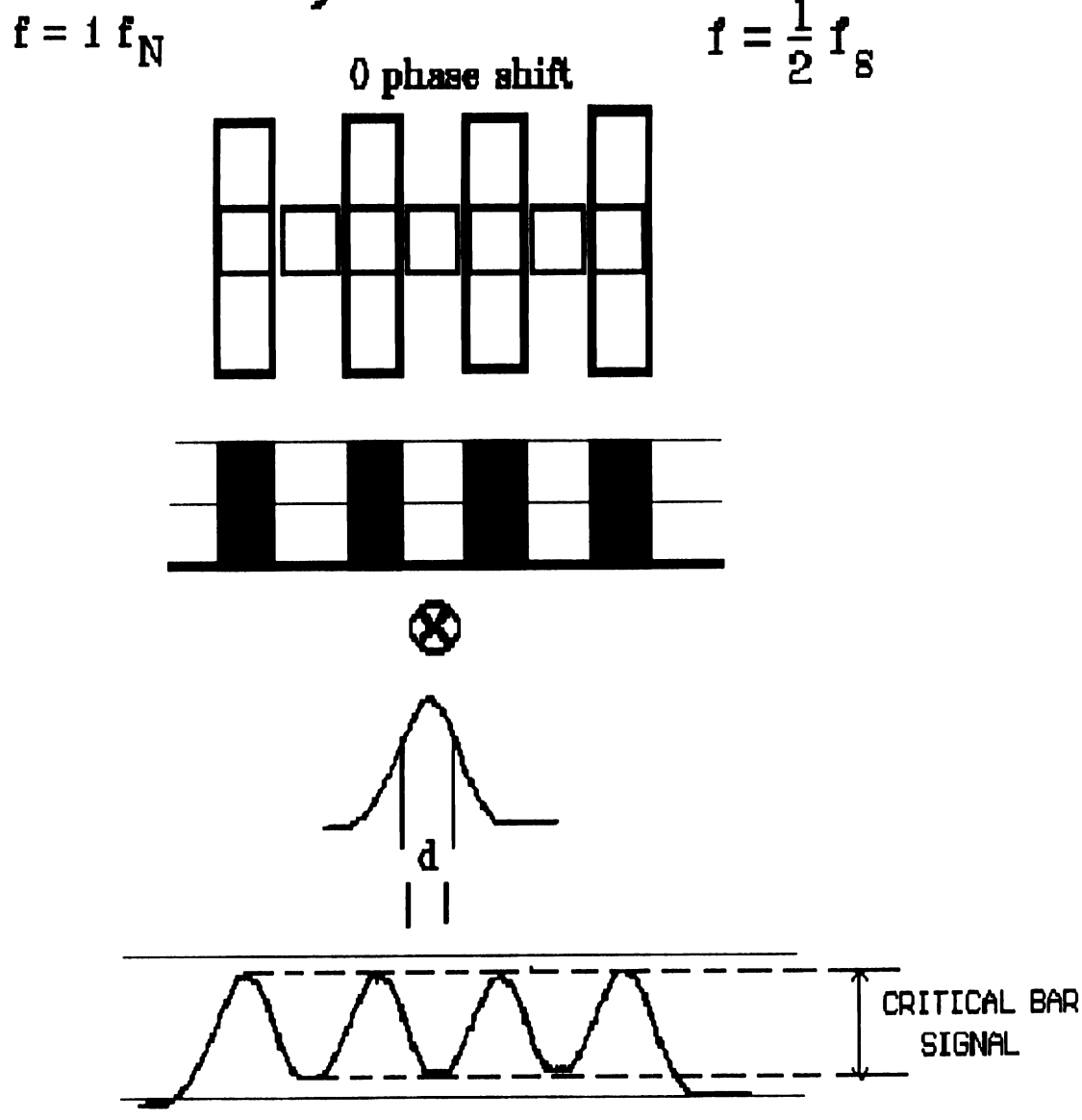

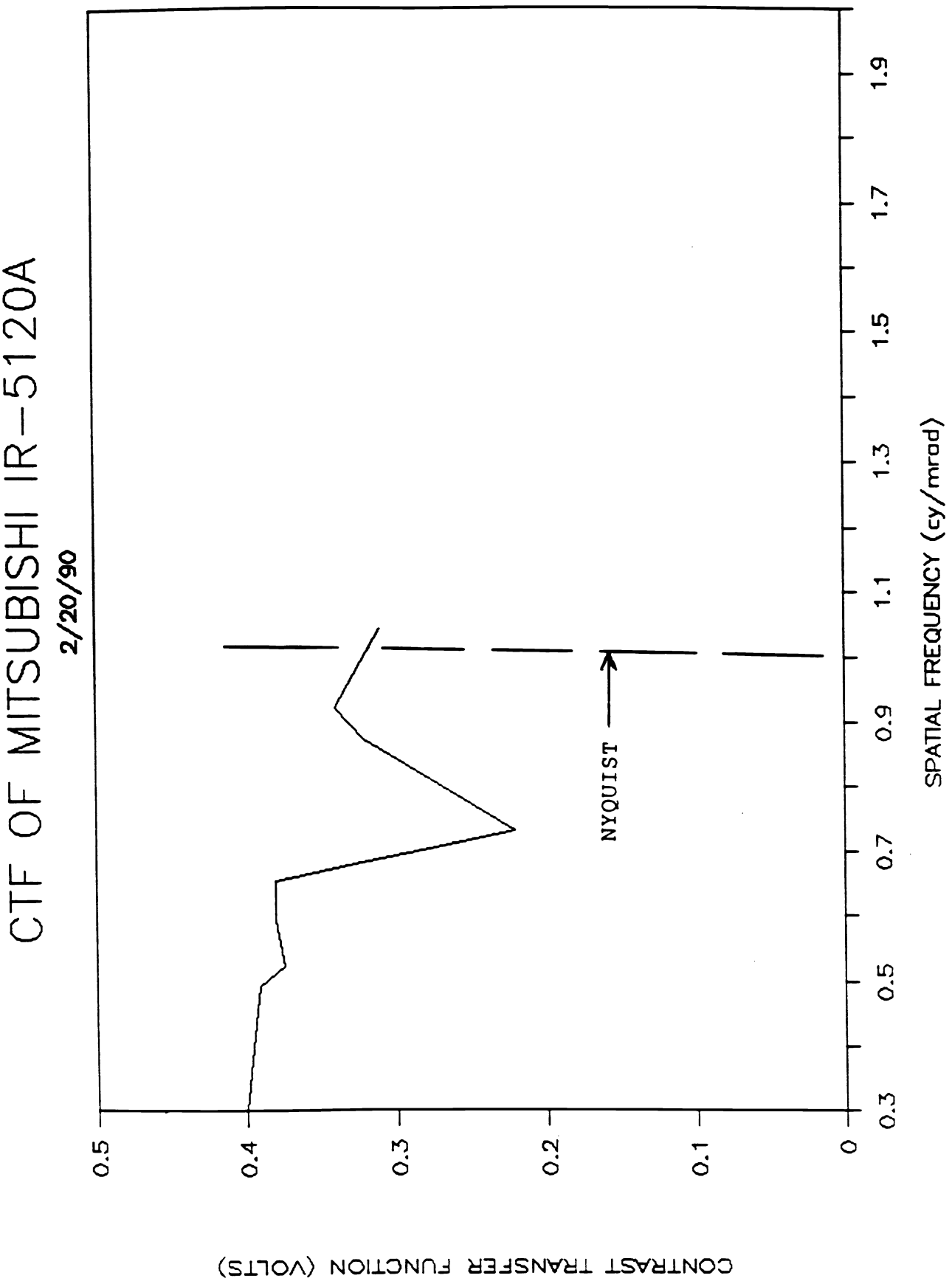
CTF OF MITSUBISHI IR-5120A
2/20/90
NYQUIST
CONTRAST TRANSFER FUNCTION (VOLTS)
SPATIAL FREQUENCY (cy/mrad)
0
0.1
0.2
0.3
0.4
0.5
0.3
0.5
0.7
0.9
1.1
1.3
1.5
1.7
1.9

Figure 5

Figure 6

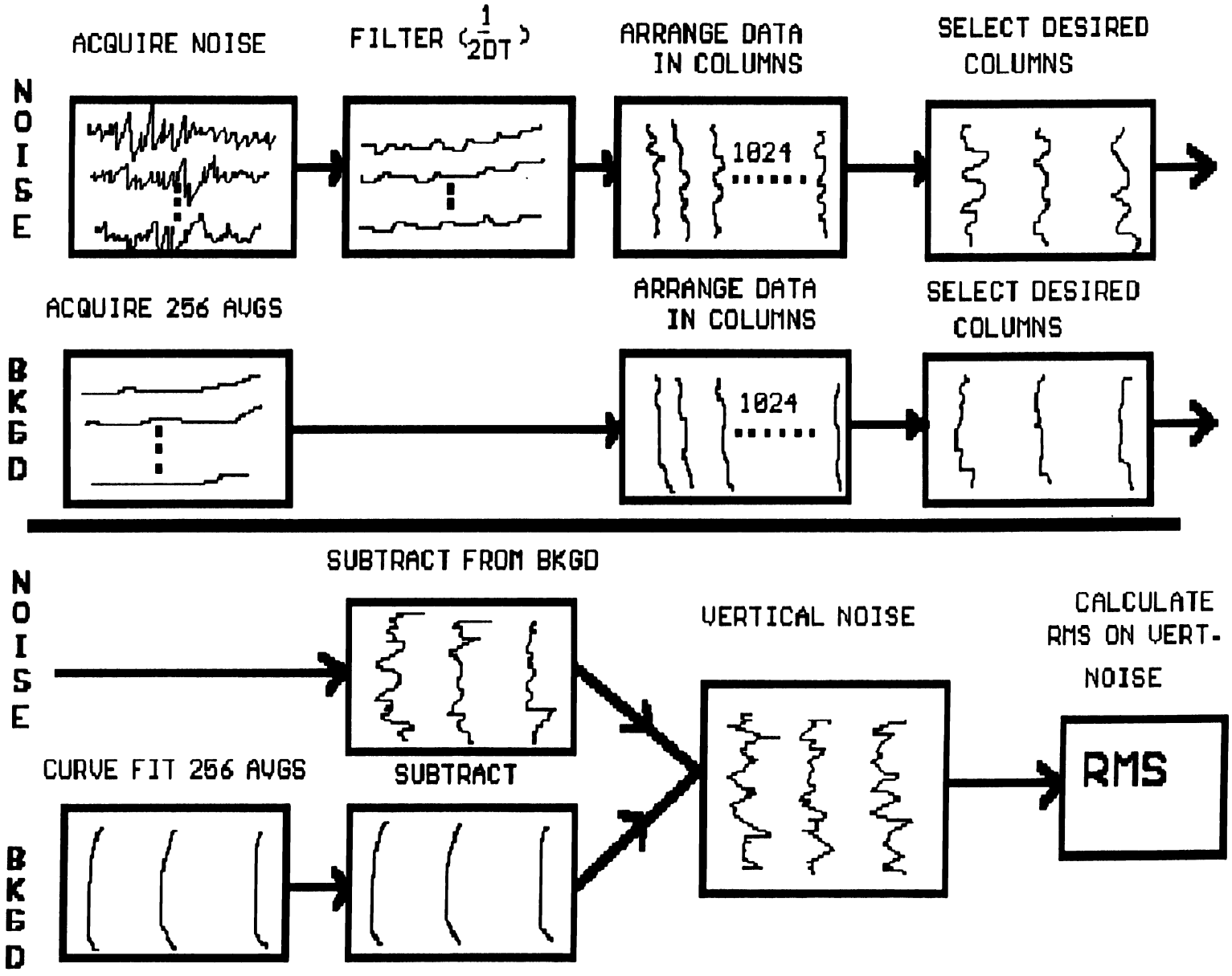
ACQUIRE NOISE
FILTER (1/2DT)
ARRANGE DATA IN COLUMNS
SELECT DESIRED COLUMNS
NOISE
1024
ACQUIRE 256 AVGS
ARRANGE DATA IN COLUMNS
SELECT DESIRED COLUMNS
BKGD
1024
SUBTRACT FROM BKGD
NOISE
VERTICAL NOISE
CALCULATE RMS ON VERT-NOISE
CURVE FIT 256 AVGS
SUBTRACT
BKGD
RMS

Figure 7

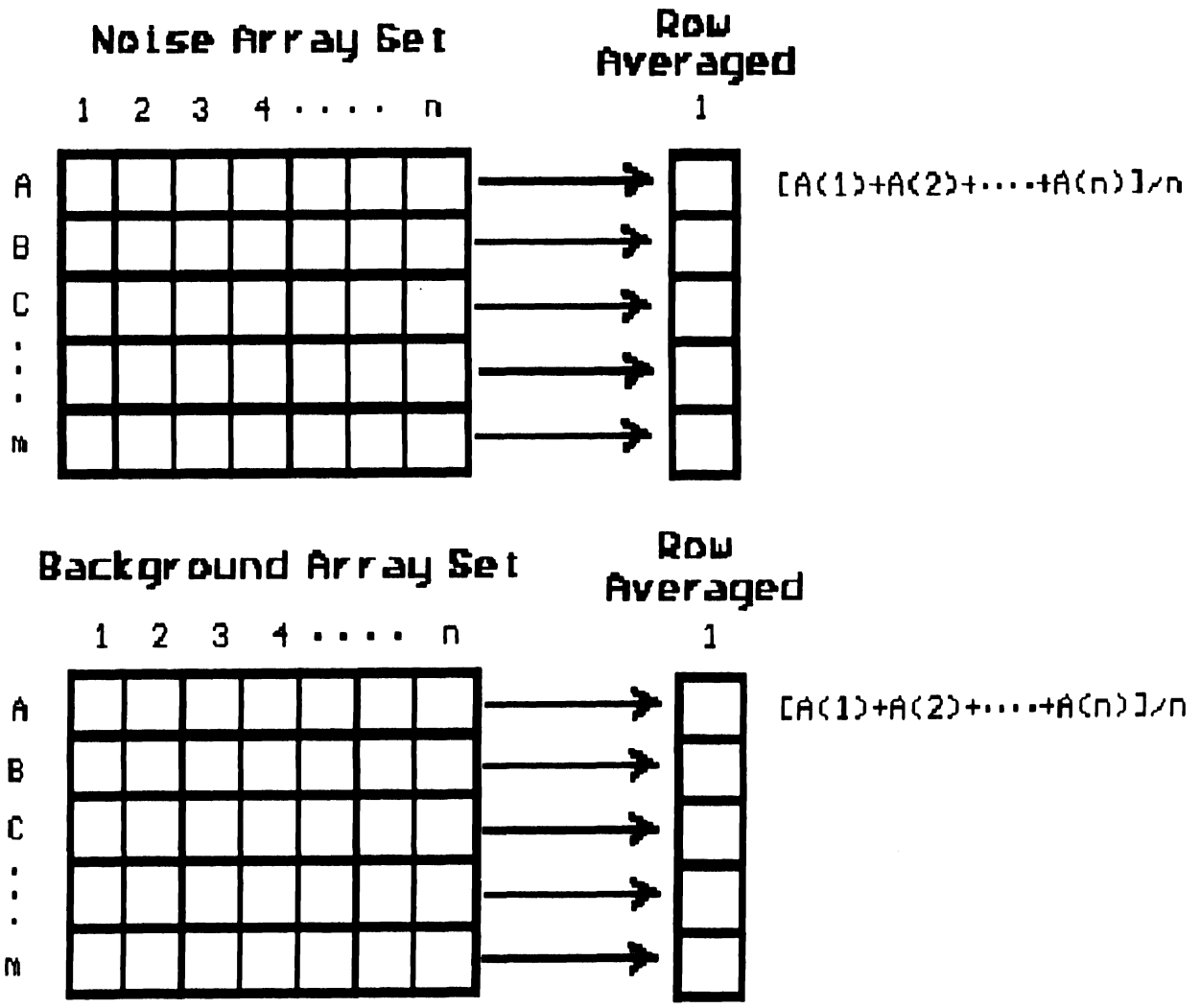
Noise Array Set
Row Averaged
1 2 3 4 · · · · n
1
A
B
C
M
[A(1)+A(2)+····+A(n)]/n
Background Array Set
Row Averaged
1 2 3 4 · · · · n
1
A
B
C
M
[A(1)+A(2)+····+A(n)]/n